Int J Clin Exp Med 2019;12(5):4735-4744
www.ijcem.com /ISSN:1940-5901/IJCEM0087305

Original Article

Protective effects of miR-19b in Parkinson's disease by inhibiting the activation of iNOS through negative regulation of p38 signaling pathways

Lin Chen, Lu Gan, Hong-Yan Zhou, Jiang-Hong Liang

Department of Internal Neurology, The Second Affiliated Hospital, University of South China, Hengyang 421000, P.R. China

Received October 25, 2018; Accepted December 9, 2018; Epub May 15, 2019; Published May 30, 2019

Abstract: Aim: This study aimed to investigate the protective effects of microRNA-19b (miR-19b) against Parkinson's disease (PD) by targeting p38 pathways. Methods: PD mice models were dealt with through overexpression or inhabitation of miR-19b and p38 signaling pathway inhibitors, separately, and a negative control group was established. Quantitative reverse-transcription polymerase chain reaction was performed to measure miR-19b and mRNAs of p38 pathway relative genes. Western blotting was utilized to measure levels of proteins with respect to p38 relative genes and generation and apoptosis for neurons. Immunohistochemistry was used to detect the activities of inducible nitric-oxide synthase (iNOS) and tyrosine hydroxylase (TH). Nissl staining method was adopted to observe the generation of Nissl bodies. Annexin V- fluorescein isothiocyanate (FITC) and propidium iodide (PI) double staining was used to measure cell apoptosis. Results: Compared with the normal group, miR-19b in the model group was decreased, but mRNA and phosphorylated proteins of p38 were significantly increased ($P < 0.05$). Compared with the negative control group, iNOS in miR-19b mimic, SB203580, and miR-19b mimic + SB203580 groups was activated. Generation of neuron cells and expression of dopamine transporter (DAT), proliferating cell nuclear antigen (PCNA), and Bcl-2 in the above three groups were significantly upregulated. Also, apoptotic neurons and expression of cleaved-caspase 3, Bax were upregulated ($P < 0.05$). Changes in the miR-19b mimic + SB203580 group were the most obvious. Conclusion: miR-19b exerts protective effects in Parkinson's by inhibiting the activation of iNOS through regulation of p38 signaling pathways.

Keywords: microRNA-19b, p38, inducible nitric-oxide synthase, Parkinson's disease, neuron

Introduction

Parkinson's disease (PD), a degenerative disease of the central nervous system, is featured by a prominent degeneration of nigrostriatal dopamine (DA) neurons. Despite clinical and preclinical studies of neuroprotective strategies for PD, there are no effective treatments preventing or slowing the progression of neurodegeneration [1]. At present, the etiology of PD remains elusive. Factors, like genes, oxidative stress, environment, and age, may participate in the degeneration process of DA neurons [2]. Autopsy results of PD patients have confirmed that inducible nitric-oxide synthase (iNOS) was highly activated in midbrain substantia nigra [3]. Jung DH et al. demonstrated that there are many glial cells expressing iNOS in the DA neurons of PD patients. The iNOS can subsequently induce large quantities of NO, which may be an important factor inducing the death of DA neurons [4].

MicroRNAs are small noncoding molecules involved in the regulation of various biological processes, such as cell proliferation, migration, invasion, and apoptosis [5]. miR-19b has been proven to exert inportant roles in the pathogenesis of various cancers, such as colorectal cancer and non-small lung cancer [6, 7]. A study designed by Marques et al. indicated that mRNA expression of miR-19b was significantly decreased in patients with neurodegenerative diseases, including PD and multiple systematrophy, indicating that miR-19b may be a diagnostic marker of PD and multiple systematr-

Table 1. Primer sequences for quantitative real-time polymerase chain reaction

Gene	Sequence (5'-3')	
miR-19b	Forward	TGTGCAAATCCATGCAAAATGA
	Reverse	GCTCACTGCAACCTCCTCCTCC
p38	Forward	TCGAGACCGTTTCAGTCCATC
	Reverse	GGGTCACCAGGTACACGTCATT
U6	Reverse	GTGCTCCTGCTTCGGCAGCACATATAC
	Forward	CGTTGACATCCGTAAAGAC
GAPDH	Reverse	CCCTTCATTGACCTCAACTAC
	Forward	CCACGACTCATACAGCACC

Note: miR-19b, microRNA-19b; GAPDH, glyceraldehyde-3-phosphate dehydrogenase

ophy [8]. It was shown that p38 signaling pathways are associated with differentiation of neural stem cells [9]. Another study further confirmed that inhibition of p38 signaling pathways revealed potential therapeutic targets for attenuation of cardinal symptoms and complications in patients with PD [10]. Regardless of the discovery of relationship between p38 signaling pathways and PD, there is insufficient information concerning their mechanisms of action. Whether p38 signaling pathways are regulated by upstream miRNA has not been fully elucidated. The present study investigated expression of miR-19b and examined its roles in PD. Results revealed that miR-19b could inhibit activation of iNOS and may be a potential target in the treatment of PD.

Materials and methods

Ethic statements

Animal use and all experimental procedures were carried out in accordance with Laboratory Animal Management Regulations. They were approved by Experimental Animal Ethics Committee of The Second Affiliated Hospital, University of South China.

Animal grouping and treatment

A total of 15 Parkinson's disease mice (C5 7BL/6N) and 3 healthy mice, aged 10-12 weeks and weighing about 21~24 g, were purchased from Guangzhou Sai Ye Biotechnology Co., Ltd. (Guangzhou, Guangdong, China). They were raised at a controlled temperature between 20 and 24°C, with relative humidity conditions of 50% to 70%. The model mice were then randomly divided into five groups, with 3 in each group: negative control group (PD mice were injected with 20 pmol NC sequence via tail veins), miR-19b mimic (PD mice were injected with 20 pmol miR-19b mimics via tail veins), miR-19b inhibitor (PD mice were injected with 20 pmol miR-19b inhibitor via tail veins), SB 203580 group (PD mice were injected with p38 signaling pathway specific inhibitor (2 mg/kg) SB203580), and miR-19b mimic + SB203580 group (PD mice were injected with miR-19b mimics and p38 signaling pathway specific inhibitor (2 mg/kg) SB203580). Sequences in this experiment were synthesized by Beijing Genomics Institute BGI. All transfection procedures were performed in accrdance with the instructions of Lipofectamine 2000 (11668-019, Invitrogen, USA).

Preparation of striatums

After 48-72 hours, the mice were anesthetized with 1% sodium pentobarbital (30 mg/kg; Sigma, CA, USA) through intraperitoneal injections. They were killed and soaked in 75% ethanol for 3 minutes to sterilize. Nigrostriatum in each group was collected through craniotomy operations and subsequently reserved at -80°C for further use.

Quantitative real-time PCR (qRT-PCR)

After striatums (stored at -80°C) were grinded and centrifuged in liquid nitrogen, total RNA was extracted using a total RNA extraction kit (Gibco-BRL, Grand Island, N.Y.). RNA was dissolved through repeated shaking. Optical density (OD) value at a wavelength of 260 nm was detected by means of a DNA/RNA tester (Beckman Coulter, Miami, FL, USA). After adjusting the concentrations of RNA, Sensiscript RT Kit (K1621; Fermentas, Maryland, NY, USA) was used to synthetize cDNA, according to manufacturer instructions. Reaction conditions were performed as follows: 70°C for 10 minutes, bathing for 2 minutes, 42°C for 60 minutes, and 70°C for 10 minutes again. The obtained cDNA were stored at -80°C for further use. The reaction was conducted according to the instructions of ABI 7500 Real-Time PCR System (ABI Company, Oyster Bay, NY, USA). Primers were designed and synthesized by the Beijing Qinke Xinye Biotechnology Ltd. (Beijing, China) (**Table 1**). The reaction liquid (total of 25 μl) included: 2×Quantiect SYBR Green PCR

12.5 μL; RNase-free water 5 μL; 0×miscript Primer Assay 140/27a/U6 5 μL; Template cDNA 2.5 μL. Reaction conditions were as follows: pre-denaturation at 95°C for 15 minutes, 40 cycles of denaturation at 94°C for 15 seconds, annealing at 55°C for 30 seconds, and extension at 70°C for 30 seconds. Glyceraldehyde-phosphate dehydrogenase (GAPDH) and U6 were used as internal references. The $2^{-\Delta\Delta CT}$ method was used to calculate relative mRNA expression levels of striatal neurons genes. The experiment was repeated three times.

Western blotting analysis

The striatums were placed in liquid nitrogen and made into homogenate, with the addition of a lysis buffer (containing 50 mmol/L Tris, 150 mmol/L NaCl, 5 mmol/L EDTA, 0.1% SDS, 1% NP-40, 5 μg/mL Aprotinin and 2 mmol/LPMSF) and protein lysate. Sample tissues were then placed at 4°C for 30 minutes and centrifuged at 1200 r/min for 20 minutes at 4°C. The liquid supernatant was collected and protein concentrations were examined using a BCA kit (20201ES76, Shanghai Yeasen Biotechnology Co. Ltd., Shanghai, China). The loading amount of protein lane was adjusted to 30 μg using deionized water. Subsequently, 10% stacking gel and sodium dodecyl sulfonate (SDS) separation gel were prepared. The sample loading buffer and the sample were mixed, boiled at 100°C for 5 minutes, ice-bathed for 1 minute, centrifuged, and added equally to each lane. Protein on the gels was subsequently transferred to the nitrocellulose membrane and sealed with 5% skim milk at 4°C overnight. Subsequently, the rabbit anti mouse polyclonal antibodies p38 (1:1000, ab31929, Abcam, Cambridge, MA, USA) , p-p38 (1:1000, ab47363, Abcam, Cambridge, MA, USA), DAT (dopamine transporter, Abcam, Cambridge, MA, USA), (1 μg/mL, ab111468, Abcam, Cambridge, MA, USA), cleaved-caspase 3 (1:5000, ab214430, Abcam, Cambridge, MA, USA), Bcl-2 associated X Protein (Bax, 1:1000, ab32503, Abcam, Cambridge, MA, USA), B-cell lymphoma-2 (Bcl-2, 1:500, ab692, Abcam, Cambridge, MA, USA), proliferating cell nuclear antigen (PCNA, 1 μg/mL, ab29, Abcam, Cambridge, MA, USA), and glyceraldehyde phosphate dehydrogenase (GAPDH, 1:10000, ab 181602, Abcam, Cambridge, MA, USA) were added for overnight incubation. PBS was used to wash the membrane 3 times at room temperature (5 min/time). The secondary HRP-labeled goat anti-rabbit antibody IgG (1:1000, Wuhan Boster Company, Wuhan, China) was then added to the membranes. The membranes were subsequently incubated at 37°C for 1 hour and washed three times with PBS (3 min/time). They were immersed in an electrochemi-luminescence (ECL) solution (Pierce, Waltham, MA, USA). Membranes were covered with a plastic wrap after removing the liquid, then exposed it in a dark room using x-rays to develop and determine color. Image J 2.0 (National Institutes of Health) was used to analyze protein bands. GAPDH was used as the internal reference and relative protein levels were calculated using the ratio between the gray value of target band and the GAPDH band. This experiment was repeated 3 times.

Immunohistochemistry

Striatum paraffin sections were prepared and added with 3% hydrogen dioxide solution after dewaxing. The slices were then incubated with rabbit anti-mouse inducible nitric-oxide synthase (iNOS, 1:600, ab3523) and tyrosine hydroxylase (TH, 1:200, ab112) at room temperature for 2 hours. The slices were then incubated with the addition of biotinylated goat anti-rabbit IgG (1:2000, ab6720, Abcam, Cambridge, MA, USA). After 30 minutes, the slices were added with 100 μL SABC solution and placed at 37°C for 20 minutes. Subsequently, the sections were washed with PBS, stained with diaminobenzidine (DAB) (P0203, Shanghai Biyuntian Biotechnology Co., Ltd., Shanghai, China), and counter-stained again with hematoxylin (SH8390, Solarbio, Britain) for 2 minutes. Sections were then soaked in saturated sodium dihydrogen phosphate and washed by water, dehydrated by ethanol, cleared in xylene, and sealed with neutral balsam. Finally, the samples were observed under a light microscope (37XF-PC, Shanghai Optical Instrument Co., Ltd., Shanghai, China). Image-pro plus 7.0 (Media Cybernetics) was used to calculate the rate of positively-stained cells.

Nissl's staining

After being dealt with polylysine, the slices of striatal neurons were dried and stored at -80°C. This was followed by hydration with PBS for 10 minutes and staining with 1% toluidine blue

(T0394, Sigma, USA) for 8 minutes. The slices were washed with distilled water for 3 minutes and hydrated with gradient ethanol (70%, 80%, 85%, 95%, and 100%, 2 min for each), cleared by xylene, and sealed by neutral balsam for observation. A fluorescence microscope (Olympus, Japan) was utilized to detect dyeing conditions. A total of six visual fields were randomly selected under a 400× objective lens. Image-pro plus 7.0 (Media Cybernetics) was used to calculate the Nissl's bodies, as well as its average value.

Apoptosis detection

The stored striatal neurons tissues were digested with 0.25% trypsin and incubated at room temperature until the cell contour became round. The sections were then added with cell culture medium, making a cell suspension. It was removed to the centrifuge tube and centrifuged at 2000 r/min for 5 minutes. The supernatant was discarded. The cells were resuspended with 1 mL PBS solution and counted. A total of 10^6 resuspended cells were selected and centrifuged at 2000 r/min for 5 minutes, then the supernatant was removed. Annexin V-FITC/PI Cell Apoptosis Detection Kit (MA0220, Meilunbio, US) was utilized to detect cell apoptosis. First, 195 μL Annexin-V-FITC buffer solution and 5μL Annexin-V-FITC were added to the cells. They were shaken and kept away from light for 15 minutes. After centrifugation at 2000 r/min for 5 minutes and discarding the supernatant, the cells were resuspended by adding 190 μL Annexin-V-FITC binding solution, stained with 10 μL propidium iodide (PI), shaken, and kept in darkness for 5 minutes. Subsequently, the FACS Calibur flow cytometer (BD company, US) was employed to detect apoptosis conditions. CellQuest3.0 (Microsoft) was utilized to analyze data and count the percentage of apoptotic cells.

Statistical analysis

SPSS 22.0 software (IBM Corp., Armonk, NY, USA) was applied for data analyses. All experiments were repeated 3 times. Measurement data are expressed as mean ± standard deviation. Comparisons between two groups were analyzed using t-test while multiple groups were analyzed using one-way analysis of variance (ANOVA). The test of normality was verified by Kolmogorov-Smirnov. Specifically, normal distribution in multiple groups was conducted by Tukey's post-hoc tests in ANOVA, whereas the non-normal distribution was conducted via post-hoc tests using Dunn's multiple comparison in Kruskal-Wallis test. $P < 0.05$ indicates statistical significance, while $P < 0.01$ indicates notable significance.

Results

miR-19b was expressed at a low level but p38 signaling pathways were activated in mice with PD. Moreover, qRT-PCR and Western blotting were performed to detect expression of miR-19b and activation of p38 signaling pathways. As shown in **Figure 1**, miR-19b expression showed a significant decline in the mice with PD, but p38 mRNA and phosphorylation protein expression were increased in PD mice, compared to normal mice (all $P < 0.05$). There were no significant differences in total p38 signaling pathway protein levels between the two groups ($P > 0.05$). Present results indicate that the declined miR-19b expression and activated p38 signaling pathways might be related to PD.

miR-19b induced inactivation of p38 signaling pathways

To explore the relationship between miR-19b and p38 signaling pathways, qRT-PCR and Western boltting were utilized to detect the activation of p38 signaling pathways after being overexpressed or inhibited by miR-19b. As shown in **Figure 2**, compared with the negative control group, p38 mRNA and p-p38 proteins were declined in the miR-19b mimic, SB203580, and miR-19b mimic + SB203580 groups, but p38 mRNA and p-p38 protein were increased in the miR-19b inhibitor group (all $P < 0.05$). There were no significant differences in levels of total p38 proteins in each group ($P > 0.05$). Results suggest that miR-19b negatively regulated p38 signaling pathways.

miR-19b inhibited expression of iNOS by inactivating p38 signaling pathways

Immunohistochemistry was performed to detect expression of striatal neurons iNOS in each group. It was found that (**Figure 3**) expression of iNOS was mainly localized in the cytoplasm and nucleus. Compared with the negative control group, expression of iNOS was

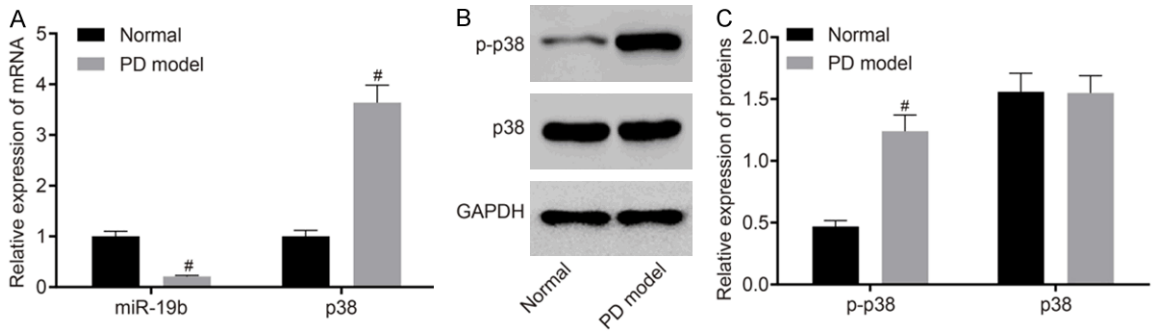

Figure 1. miR-19b was robustly decreased and p38 signaling pathways were significantly activated in PD mice. Note: A. The histogram showing miR-19b expression and mRNA expression of p38; B. Protein bands of p-p38, p38, and GAPDH; C. Histogram showing the relative protein level of p-p38 and p38. #, $P < 0.05$ compared with the negative control group; n=15 in the model group while n=3 in the normal group. Measurement data are expressed as the mean ± standard deviation (SD) and were analyzed using t-test. The experiment was repeated 3 times.

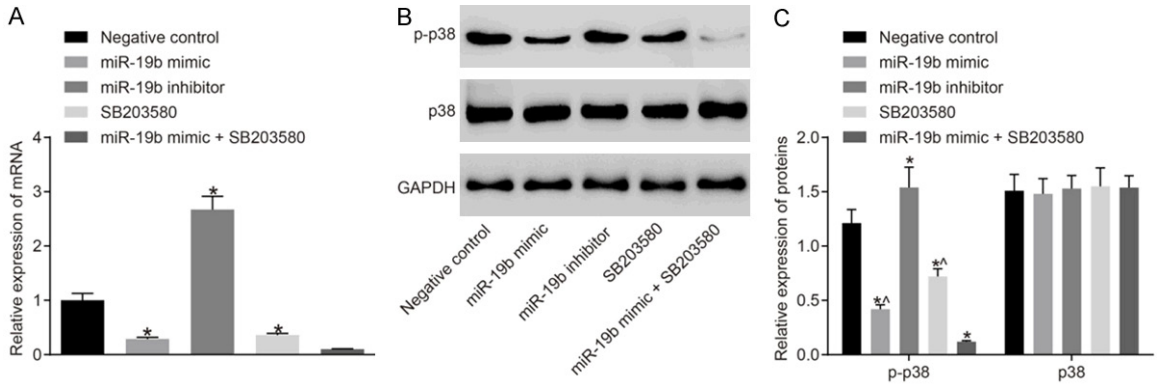

Figure 2. miR-19b inhibited activation of p38 signaling pathways. Note: A. qRT-PCR was used to detect relative expression of p38 mRNA; B. Protein bands of p-p38, p38, and GAPDH in each group; C. Histogram showing the relative protein level of p-p38 and p38 in each group; *, $P < 0.05$ compared with the negative control group; ^, $P < 0.05$ compared with the miR-19b mimic + SB203580 group. All n=3 in the each group. Measurement data are expressed as the mean ± standard deviation (SD) and were analyzed using one-way ANOVA. The testing of each group was conducted in triplicate.

significantly decreased in the miR-19b mimic, SB203580, and miR-19b mimic + SB203580 groups, but significantly increased in the miR-19b inhibitor group. In addition, expression of iNOS was significantly increased in the miR-19b mimic and SB203580 groups, compared to the miR-19b mimic + SB203580 group (all $P < 0.05$). Results suggest that overexpression of miR-19b could inhibit iNOS expression by inactivating p38 signaling pathways.

miR-19b induced neuron generation but inhibited apoptosis by inactivating p38 signaling pathways

qRT-PCR and Western blotting were utilized, respectively, to detect mRNA and protein expression of DAT, PCNA, and apoptosis-related factors. As shown in **Figure 4**, compared with the negative control group, the miR-19b mimic, SB203580, and miR-19b mimic + SB203580 groups showed high mRNA and protein levels of DAT, PCNA, and Bcl-2, but low levels of cleaved-caspase 3 and Bax. The miR-19b inhibitor group showed decreased mRNA and protein levels of DAT, PCNA, and Bcl-2, but increased levels of cleaved-caspase 3 and Bax (all $P < 0.05$). Compared with the miR-19b mimic + SB203580 group, mRNA and protein levels of DAT, PCNA, and Bcl-2 were significantly decreased in miR-19b mimic group and SB203580 group, but levels of cleaved-caspase 3 and Bax were significantly increased in all groups (all $P < 0.05$).

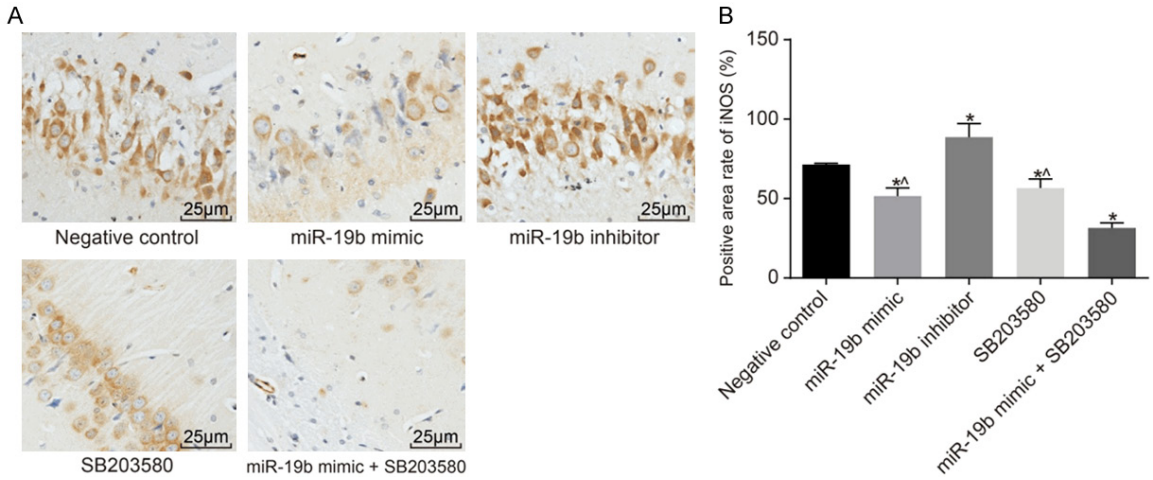

Figure 3. iNOS expression of striatums by immunohistochemistry. Note: A. The results of Immunohistochemistry; B. Positive expression of iNOS in striatal neurons in each group; *, $P < 0.05$ compared with the negative control group; ^, $P < 0.05$ compared with the miR-19b mimic + SB203580 group. All n=3 in each group. Measurement data are expressed as the mean ± standard deviation (SD) and were analyzed using one-way ANOVA. The testing of each group was repeated 3 times.

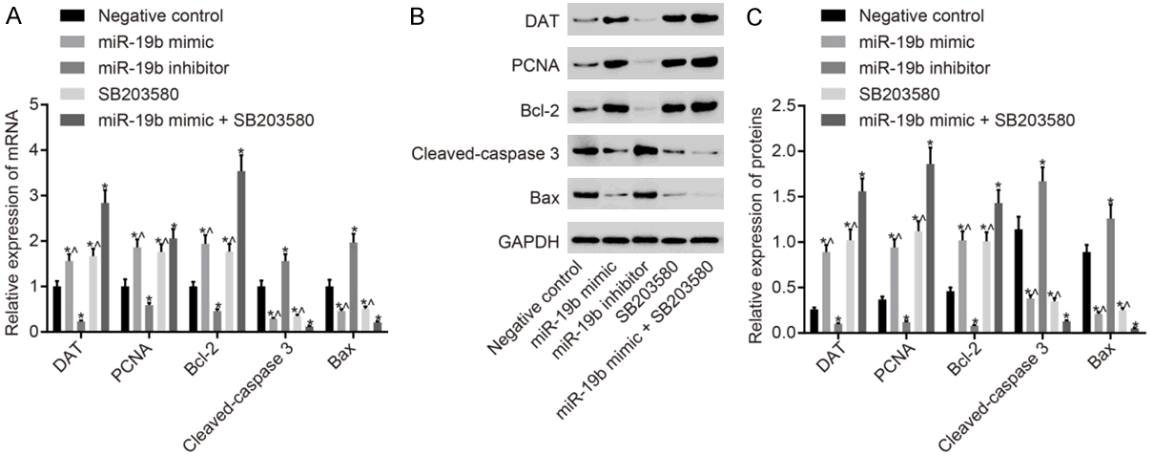

Figure 4. Relative levels of DAT, PCNA, Bcl-2, cleaved-caspase 3, and Bax. Note: A. The histogram showing mRNA expression of DAT, PCNA, Bcl-2, cleaved-caspase 3, and Bax in each group; B. Protein bands of DAT, PCNA, Bcl-2, cleaved-caspase 3, and Bax in each group; C. Histogram showing the relative protein level of DAT, PCNA, Bcl-2, cleaved-caspase 3, and Bax in each group. *, $P < 0.05$ compared with the negative control group; ^, $P < 0.05$ compared with the miR-19b mimic + SB203580 group. All n=3 in the each group. Measurement data are expressed as the mean ± standard deviation (SD) and were analyzed using one-way ANOVA. The testing of each group was conducted in triplicate.

miR-19b induced neuron generation and TH expression by inhibiting activation of p38 signaling pathways

Immunohistochemistry and Nissl staining were used to measure levels of TH (**Figures 5** and **6**). It was found that TH was expressed both in the cytoplasm and nucleus. Compared with the negative control group, expression of TH and the number of neurons were significantly increased in the miR-19b mimic, SB203580, and miR-19b mimic + SB203580 groups, but significantly declined in the miR-19b inhibitor group. At the same time, expression of TH and the numbers of neurons were significantly declined in the miR-19b mimic and SB203580 groups, compared to the miR-19b mimic + SB203580 group (all $P < 0.05$). Results obtained from the above experiments indicate that miR-19b induced neurons generation and

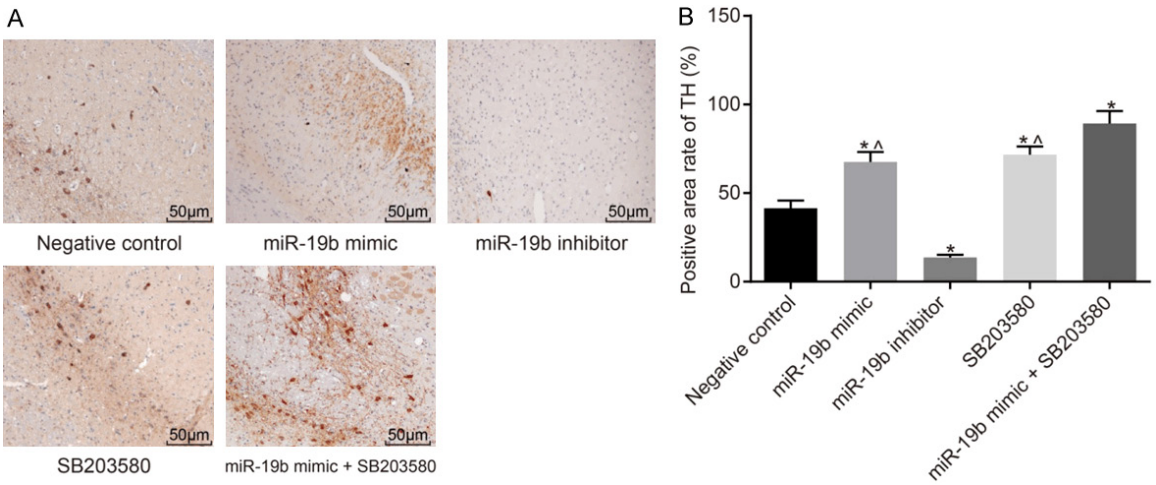

Figure 5. Immunohistochemistry suggests that miR-19b could induce the generation of neurons. Note: A. The results of Immunohistochemistry in each group; B. Histogram showing the positive expression of TH in each group; *, $P < 0.05$ compared with the negative control group; ^, $P < 0.05$ compared with the miR-19b mimic + SB203580 group. All n=3 in the each group. Measurement data are expressed as the mean ± standard deviation (SD) and were analyzed using one-way ANOVA. The testing of each group was conducted 3 times.

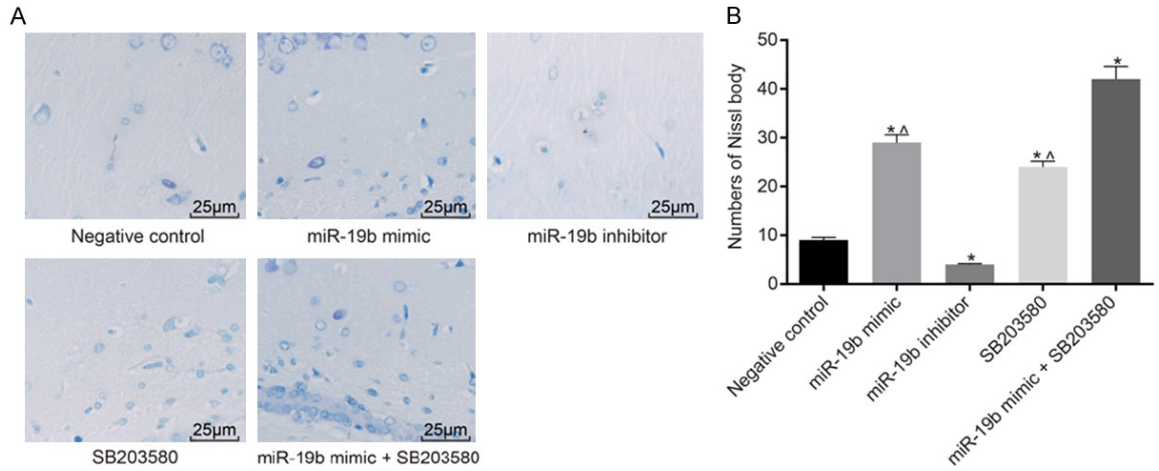

Figure 6. Nissl staining indicates that miR-19b could induce the generation of neurons. Note: A. Images of Nissl staining in each group; B. Numbers of Nissl body in each group's striatums; *, $P < 0.05$ compared with the negative control group; ^, $P < 0.05$ compared with the miR-19b mimic + SB203580 group. All n=3 in the each group. Measurement data are expressed as the mean ± standard deviation (SD) and were analyzed using one-way ANOVA. The testing of each group was conducted in triplicate.

TH expression through inhibiting activation of p38 signaling pathways.

miR-19b inhibited neuron apoptosis through negative regulation of p38 signaling pathways

Annexin V- fluorescein isothiocyanate (FITC), combined with propidium iodide (PI) double staining and flow cytometry, were used to measure striatal neuron apoptosis in each group. As shown in **Figure 7**, compared with the negative control group, the apoptosis rate was significantly decreased in the miR-19b mimic, SB203580, and miR-19b mimic + SB203580 groups, but significantly increased in the miR-19b inhibitor group (all $P < 0.05$). Effects from the combined treatment of miR-19b mimics and SB203580 were much more significant in inhibiting apoptosis, compared to the miR-19b mimic group and SB203580 group (all $P <$

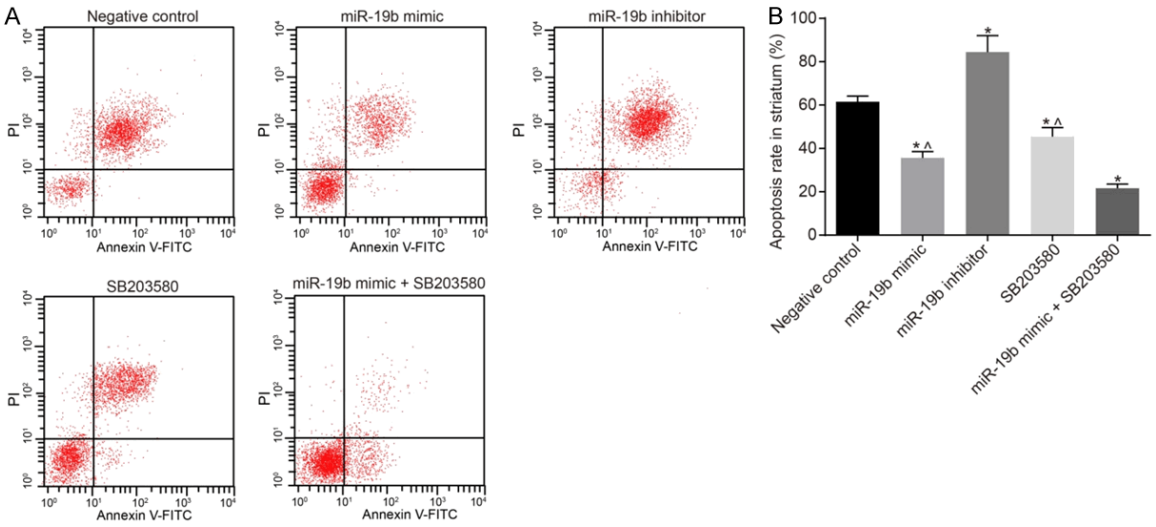

Figure 7. Flow cytometry indicates that miR-19b could inhibit cell apoptosis in the striatum. A. Images of flow cytometry in each group; B. Histogram showing the cell apoptosis in striatum in each group; *, $P < 0.05$ compared with the negative control group; ^, $P < 0.05$ compared with the miR-19b mimic + SB203580 group. Measurement data are expressed as the mean ± standard deviation (SD) and were analyzed using one-way ANOVA. The test of each group was repeated 3 times.

0.05). Results suggest that miR-19b could inhibit neuron apoptosis by inactivating p38 signaling pathways.

Discussion

The degeneration of dopaminergic (DA) neurons has been recognized as a central event contributing to the pathogenesis of PD [11, 12]. As a neurodegenerative disease, PD is common among the elderly. Environmental factors, genetic factors, and mitochondrial dysfunction are widely regarded as the common causes of PD [13]. Accumulating evidence has indicated that miRNAs also play an important role in patients with PD. There is an obvious imbalance of miRNA distribution in the dopaminergic neurons of PD patients [14]. Hence, it is of vital importance to understand the underlying pathological mechanisms related to PD, discovering novel diagnostic biomarkers and therapeutic strategies for PD. Present findings provide evidence that miR-19b inhibits expression of iNOS and promotes the generation of neuron via p38 signaling pathways in PD.

Initially, miR-19b was determined to be lowly expressed in the striatum of mice with PD. Expression of p38 mRNA and phosphorylated proteins showed an opposite trend. qRT-PCR and Western blotting were further utilized to identify the relationship between miR-19b and p38 signaling pathways. Results suggest that activation of p38 signaling pathways was negatively regulated by miR-19b. Cao XY et al. confirmed that expression of miR-19b in serum of PD patients was significantly decreased by analyzing differentially expressed miRNA between PD patients and healthy individuals [15]. Results obtained from an exploratory study by Bottaorfila also stressed this point. They found that downregulated levels of specific circulating serum miRNAs were associated with PD and that miR-19b could be used as a noninvasive biomarker for PD [16]. Oxidative stress has been confirmed to be an important factor in the pathogenesis of various neurodegenerative diseases, including PD [17]. Reactive oxygen species (ROS) is one of the necessities for cells in the process of normal metabolism, but once the secretion of ROS is excessive, it is very easy to accelerate the degradation of key molecules, such as lipids and proteins, in the human body, negatively impacting the integration and function of cells [18]. The p38 signaling pathway, an important branch of MAPK signaling pathways, has been proven to play a regulatory role in the oxidative stress of many kinds of cells [19]. A study designed by Xu H found that PC12 cells showed significant apoptosis after activation of p38 signaling pathways, suggesting p38 signaling pathways are involved in the regulation of neuronal apoptosis [20]. The present study

detected expression of miR-19b and activation of p38 signaling pathways, confirming that downregulation of miR-19b and activation of the p38 signaling pathways may be related to the pathogenesis of PD.

A study performed by Gong X et al. found that activation of p38 signaling pathways could induce iNOS activation in renal tubular epithelial cells and led to renal tubule injury [21]. Ren B confirmed that iNOS positive cells were mainly expressed in the nigra of PD patients and its excessive expression was an important contributor to degeneration of DA neurons. Inhibition of iNOS expression could reduce the degeneration of DA neurons in PD patients [22]. Similarly, the present study found that overexpression of miR-19b promoted the inactivation of p38 signaling pathways and reduced expression of iNOS in the nigra of PD mice. Dopamine transporter (DAT) is an important marker of DA neurons. Its content is directly related to the number, as well as the function, of DA neurons in striatums [23, 24]. Proliferating cell nuclear antigen (PCNA) functions in DNA replication, repair, and recombination, as a sliding clamp for various DNA replication polymerases and a scaffold for many DNA repair and recombination enzymes [25]. In recent years, studies have proven that PCNA was closely related to the repair of nerve injury and had the ability to effectively reflect the proliferation activity of neural cells [26, 27]. Furthermore, it was found that, compared with the negative control group, miR-19b mimic group and SB203580 groups showed significantly upregulated levels of DAT, PCNA, and Bcl-2, but decreased levels of cleaved-caspase 3 and Bax. The combination group was more obvious than the other groups. Detection for TH and neuron growth also further confirmed that miR-19b could significantly inhibit activation of p38 signaling pathways, protecting the neurons of PD mice.

In conclusion, present data suggests that miR-19b could inhibit activation of iNOS and promote neuronal production in PD patients through the negative regulation of p38 signaling pathways. Therefore, miR-19b could potentially function as a biomarker for the prognosis of PD, as well as a therapeutic target for PD treatment. However, more experiments should be conducted in the future to further elucidate the underlying mechanisms of miR-19b in PD.

Acknowledgements

This work was supported by 2014 Hunan Medical and Health Scientific Research Project (B2014-056).

Disclosure of conflict of interest

None.

Address correspondence to: Lin Chen, Department of Internal Neurology, The Second Affiliated Hospital, University of South China, No. 35 Jiefang Road, Huaxin District, Hengyang 421000, P.R. China. Tel: 0734-8185696; E-mail: chenlin421000@163.com

References

[1] Sonsalla PK, Wong LY, Harris SL, Richardson JR, Khobahy I, Li W, Gadad BS and German DC. Delayed caffeine treatment prevents nigral dopamine neuron loss in a progressive rat model of Parkinson's disease. Exp Neurol 2012; 234: 482-487.

[2] Noyce AJ, Bestwick JP, Silveira-Moriyama L, Hawkes CH, Giovannoni G, Lees AJ and Schrag A. Meta-analysis of early nonmotor features and risk factors for Parkinson disease. Ann Neurol 2012; 72: 893-901.

[3] Khasnavis S, Ghosh A, Roy A and Pahan K. Castration induces Parkinson disease pathologies in young male mice via inducible nitric-oxide synthase. J Biol Chem 2013; 288: 20843-20855.

[4] Jung DH, Kim KH, Byeon HE, Park HJ, Park B, Rhee DK, Um SH and Pyo S. Involvement of ATF3 in the negative regulation of iNOS expression and NO production in activated macrophages. Immunol Res 2015; 62: 35-45.

[5] Minones-Moyano E, Porta S, Escaramis G, Rabionet R, Iraola S, Kagerbauer B, Espinosa-Parrilla Y, Ferrer I, Estivill X and Marti E. MicroRNA profiling of Parkinson's disease brains identifies early downregulation of miR-34b/c which modulate mitochondrial function. Hum Mol Genet 2011; 20: 3067-3078.

[6] Cruz-Gil S, Sanchez-Martinez R, Gomez de Cedron M, Martin-Hernandez R, Vargas T, Molina S, Herranz J, Davalos A, Reglero G and Ramirez de Molina A. Targeting the lipid metabolic axis ACSL/SCD in colorectal cancer progression by therapeutic miRNAs: miR-19b-1 role. J Lipid Res 2018; 59: 14-24.

[7] Zhu J, Wang S, Chen Y, Li X, Jiang Y, Yang X, Li Y, Wang X, Meng Y, Zhu M, Ma X, Huang C, Wu R, Xie C, Geng S, Wu J, Zhong C and Han H. miR-19 targeting of GSK3beta mediates sul-

foraphane suppression of lung cancer stem cells. J Nutr Biochem 2017; 44: 80-91.
[8] Marques TM, Kuiperij HB, Bruinsma IB, van Rumund A, Aerts MB, Esselink RAJ, Bloem BR and Verbeek MM. MicroRNAs in cerebrospinal fluid as potential biomarkers for Parkinson's disease and multiple system atrophy. Mol Neurobiol 2017; 54: 7736-7745.
[9] Hu JG, Wang YX, Wang HJ, Bao MS, Wang ZH, Ge X, Wang FC, Zhou JS and Lu HZ. PDGF-AA mediates B104CM-induced oligodendrocyte precursor cell differentiation of embryonic neural stem cells through Erk, PI3K, and p38 signaling. J Mol Neurosci 2012; 46: 644-653.
[10] Wang G, Pan J and Chen SD. Kinases and kinase signaling pathways: potential therapeutic targets in Parkinson's disease. Prog Neurobiol 2012; 98: 207-221.
[11] Trinh K, Moore K, Wes PD, Muchowski PJ, Dey J, Andrews L and Pallanck LJ. Induction of the phase II detoxification pathway suppresses neuron loss in drosophila models of Parkinson's disease. J Neurosci 2008; 28: 465-472.
[12] Franco-Iborra S, Vila M and Perier C. The Parkinson disease mitochondrial hypothesis: where are we at? Neuroscientist 2016; 22: 266-277.
[13] Guo JD, Zhao X, Li Y, Li GR and Liu XL. Damage to dopaminergic neurons by oxidative stress in Parkinson's disease (Review). Int J Mol Med 2018; 41: 1817-1825.
[14] Briggs CE, Wang Y, Kong B, Woo TU, Iyer LK and Sonntag KC. Midbrain dopamine neurons in Parkinson's disease exhibit a dysregulated miRNA and target-gene network. Brain Res 2015; 1618: 111-121.
[15] Cao XY, Lu JM, Zhao ZQ, Li MC, Lu T, An XS and Xue LJ. MicroRNA biomarkers of Parkinson's disease in serum exosome-like microvesicles. Neurosci Lett 2017; 644: 94-99.
[16] Botta-Orfila T, Morato X, Compta Y, Lozano JJ, Falgas N, Valldeoriola F, Pont-Sunyer C, Vilas D, Mengual L, Fernandez M, Molinuevo JL, Antonell A, Marti MJ, Fernandez-Santiago R and Ezquerra M. Identification of blood serum micro-RNAs associated with idiopathic and LRRK2 Parkinson's disease. J Neurosci Res 2014; 92: 1071-1077.
[17] Gunjima K, Tomiyama R, Takakura K, Yamada T, Hashida K, Nakamura Y, Konishi T, Matsugo S and Hori O. 3, 4-dihydroxybenzalacetone protects against Parkinson's disease-related neurotoxin 6-OHDA through Akt/Nrf2/glutathione pathway. J Cell Biochem 2014; 115: 151-160.
[18] Lan AP, Chen J, Chai ZF and Hu Y. The neurotoxicity of iron, copper and cobalt in Parkinson's disease through ROS-mediated mechanisms. Biometals 2016; 29: 665-678.
[19] Watanabe T, Sekine S, Naguro I, Sekine Y and Ichijo H. Apoptosis signal-regulating kinase 1 (ASK1)-p38 pathway-dependent cytoplasmic translocation of the orphan nuclear receptor NR4A2 Is required for oxidative stress-induced necrosis. J Biol Chem 2015; 290: 10791-10803.
[20] Xu H, Wu B, Jiang F, Xiong S, Zhang B, Li G, Liu S, Gao Y, Xu C, Tu G, Peng H, Liang S and Xiong H. High fatty acids modulate P2X (7) expression and IL-6 release via the p38 MAPK pathway in PC12 cells. Brain Res Bull 2013; 94: 63-70.
[21] Gong X, Celsi G, Carlsson K, Norgren S and Chen M. N-acetylcysteine amide protects renal proximal tubular epithelial cells against iohexol-induced apoptosis by blocking p38 MAPK and iNOS signaling. Am J Nephrol 2010; 31: 178-188.
[22] Ren B, Zhang YX, Zhou HX, Sun FW, Zhang ZF, Wei Z, Zhang CY and Si DW. Tanshinone IIA prevents the loss of nigrostriatal dopaminergic neurons by inhibiting NADPH oxidase and iNOS in the MPTP model of Parkinson's disease. J Neurol Sci 2015; 348: 142-152.
[23] de la Fuente-Fernandez R. Role of DaTSCAN and clinical diagnosis in Parkinson disease. Neurology 2012; 78: 696-701.
[24] Pellecchia MT, Picillo M, Santangelo G, Longo K, Moccia M, Erro R, Amboni M, Vitale C, Vicidomini C, Salvatore M, Barone P and Pappata S. Cognitive performances and DAT imaging in early Parkinson's disease with mild cognitive impairment: a preliminary study. Acta Neurol Scand 2015; 131: 275-281.
[25] Lee KY, Yang K, Cohn MA, Sikdar N, D'Andrea AD and Myung K. Human ELG1 regulates the level of ubiquitinated proliferating cell nuclear antigen (PCNA) through Its interactions with PCNA and USP1. J Biol Chem 2010; 285: 10362-10369.
[26] Glaser S, Meng F, Han Y, Onori P, Chow BK, Francis H, Venter J, McDaniel K, Marzioni M, Invernizzi P, Ueno Y, Lai JM, Huang L, Standeford H, Alvaro D, Gaudio E, Franchitto A and Alpini G. Secretin stimulates biliary cell proliferation by regulating expression of microRNA 125b and microRNA let7a in mice. Gastroenterology 2014; 146: 1795-1808 e1712.
[27] Deng X, Wei H, Lou D, Sun B, Chen H, Zhang Y and Wang Y. Changes in CLIP3 expression after sciatic nerve injury in adult rats. J Mol Histol 2012; 43: 669-679.